Applied Physics Letters ARTICLE scitation.org/journal/apl

Wideband electromagnetic dynamic acoustic transducers (WEMDATs) for air-coupled ultrasonic applications

Cite as: Appl. Phys. Lett. **114**, 053505 (2019); doi: 10.1063/1.5086383
Submitted: 20 December 2018 · Accepted: 18 January 2019 ·
Published Online: 6 February 2019

Lei Kang, Andrew Feeney, and Steve Dixon[a)]

AFFILIATIONS

Department of Physics, University of Warwick, Coventry CV4 7AL, United Kingdom

[a)]Email: s.m.dixon@warwick.ac.uk

ABSTRACT

Achieving sufficient energy transmission over a wide frequency range is a challenge which has restricted the application of many types of air-coupled ultrasonic transducers. Conventional transducer configurations such as the piezoelectric micromachined or flexural ultrasonic transducers can be considered as narrowband. This study reports a type of ultrasonic transducer, the wideband electromagnetic dynamic acoustic transducer (WEMDAT), which operates through a combination of electromagnetic induction and Lorentz force with dynamic behaviour of a micro-scale-thick conductive film. WEMDAT prototypes have been designed, fabricated, and tested, showing their compatibility with both low and high power inputs, operating efficiently as a wideband transmitter from 46.4 kHz to 144.6 kHz with a good directivity. The WEMDAT has also been shown to operate effectively as a wideband ultrasonic receiver through the measurement in a pitch-catch configuration. The WEMDAT prototypes possess an adjustable drive coil lift-off distance from the active membrane, providing flexibility for optimizing the sensitivity of the transducers for different input levels. The performance of the WEMDATs can be optimized, showing significant potential for air-coupled ultrasonic applications.

The vibration characteristics of air-coupled ultrasonic transducers, such as piezoelectric ultrasonic transducers with matching layers, piezoelectric micromachined ultrasonic transducers (PMUTs), and flexural ultrasonic transducers (FUTs), are typically governed by the resonance modes of either the piezoelectric ceramics or the elastic plates which are used in their construction.[1–4] These transducers are by their nature narrowband devices, although they can be operated at a number of different discrete frequencies. A wideband response is highly advantageous for various applications including distance measurements, ultrasonic communication, material characterization, and non-destructive evaluation.[4–7] Principally, reliable energy transmission over a sufficiently large frequency range can be achieved through a device exhibiting a wide bandwidth of operation. In practice, the dynamic characteristics of ultrasonic transducers can be investigated through the simultaneous transmission and detection of ultrasound waves, which is essential for applications requiring an accurate time-of-flight measurement, such as in flow meters. A reliable time-of-flight-measurement can be achieved using a wideband ultrasonic transducer, since its ultrasonic response signal can be a form of sharp pulse with a short temporal length, thereby enabling the distance measurement with accuracy. It is also possible to generate complex forms of transmitting signals using a coded excitation technique to improve the signal-to-noise ratio (SNR) and the resolution of ultrasonic imaging systems.[8,9]

There are reports investigating improvements to the bandwidth performance of air-coupled ultrasonic transducers, including applying biased voltage to PMUTs, utilizing multi-frequency piezoelectric arrays, exploiting the non-resonant vibration of electromechanical films, and utilizing capacitive ultrasonic transducers and capacitive micromachined ultrasonic transducers (CMUTs).[10–14] However, challenges persist due to the necessary compromise between bandwidth, frequency-response, sensitivity, directivity, cost, complexity, robustness, operation temperature, and intrinsic safety of the transducers

in various applications. Previous research demonstrated the general concept of Lorentz-force based flexural ultrasonic transducers.[15] Three types of electromagnetically driven FUTs were fabricated, where it was shown that coupling an alternating electromagnetic field with an edge-clamped conductive plate can effectively generate and receive ultrasound in air in a narrowband frequency range dominated by the resonance frequencies of the plate. A type of air-coupled ultrasonic transducer, the wideband electromagnetic dynamic acoustic transducer (WEMDAT), has been developed based on this fundamental research.

The mechanism by which a WEMDAT generates ultrasound waves in air is illustrated in Fig. 1. An edge-clamped non-magnetic conductive foil, whose lateral dimensions are significantly greater than its thickness, is placed in an in-plane radial static magnetic field $B_{s,in}$ in the vicinity of a solenoid carrying an alternating current J_c. When the alternating current with a frequency of f_0 is delivered to the solenoid, a dynamic electromagnetic field is generated which induces an eddy current J_e in the conductive foil, as described by Faraday's law of induction. The eddy current is primarily distributed in the foil directly under the solenoid. The interaction between the eddy current J_e and the in-plane radial static magnetic field $B_{s,in}$ generates a Lorentz force $F_{L,s}$, resulting in an out-of-plane oscillation of electrons in the skin-depth area. The oscillating electrons exchange momentum with the metal atoms of the foil and thus produce an out-of-plane vibration of the foil, generating an ultrasonic wave. The thickness t of the foil is small, typically below 50 μm, much smaller than the diameter D. Thus, the vibration behaviour of the foil is much closer to that of a membrane than a plate and can have a wideband-frequency response of vibration.[16] Consequently, the foil can be driven by the Lorentz force in a relatively wide frequency range, efficiently converting electromagnetic energy into mechanical energy.

In addition to $F_{L,s}$, there is another Lorentz force $F_{L,d}$ due to the dynamic magnetic field $B_{d,in}$ generated by the driving current J_c. According to Maxwell's equations, $F_{L,d}$ is proportional to the square of J_c whilst $F_{L,s}$ is proportional to the product of J_c and $B_{s,in}$. The frequency of $F_{L,d}$ is double that of f_0, whilst the frequency of $F_{L,s}$ is the same as that of f_0. The influence of $F_{L,d}$ is much smaller than that of $F_{L,s}$ when the driving current is small and the static magnetic field is strong.[17] As soon as the conductive foil starts vibrating in the static magnetic field, an additional eddy current will be induced, generating a magnetic field which opposes the static magnetic field, as described by Lenz's law. As a consequence, a dragging force F_{drag} preventing the vibration of the foil is generated, functioning as an eddy current brake converting kinetic energy into heat.[18] This self-adaptive dragging force is proportional to the vibration velocity of the foil, beneficial for reducing the temporal duration of the ring-down vibration of the foil in transmission.

WEMDATs can operate as an ultrasound sensor as well as a transmitter. Unlike conventional air-coupled ultrasonic transducers, such as flexural ultrasonic transducers, which depend on plate vibration modes or ultrasonic transducers with matching layers, the mass of the thin conductive foil in a WEMDAT is relatively low, enabling it to efficiently gain momentum and vibrate in response to a compressional ultrasound wave. The conductive foil can be easily deformed and displaced by fluid-borne compressional waves, over a relatively wide frequency range, where its out-of-plane vibration in an in-plane static magnetic field induces an eddy current, generating a dynamic magnetic field in the solenoid. The properties of the ultrasonic wave, including frequency, amplitude, envelope, phase, and time-of-flight, can be determined through the measurement of the voltage across the solenoid.

The assembly schematic of a WEMDAT is shown in Fig. 2. Key transducer components include an annular magnet and a threaded cylindrical magnetic core with a solenoid fixed to the end, a steel backplate, and non-magnetic conductive foil which are positioned to form a cavity inside the magnet, and a vent is included in the side wall to ensure equalized pressure between the inside and the outside of the transducer, enabling operation at high and varying pressure levels.

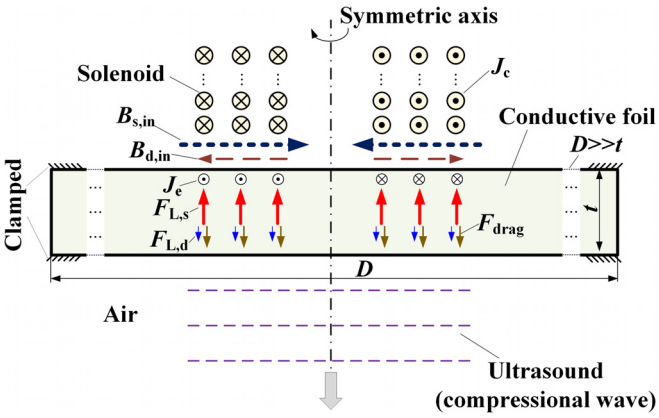

FIG. 1. Schematic diagram of ultrasound wave generation by a WEMDAT.

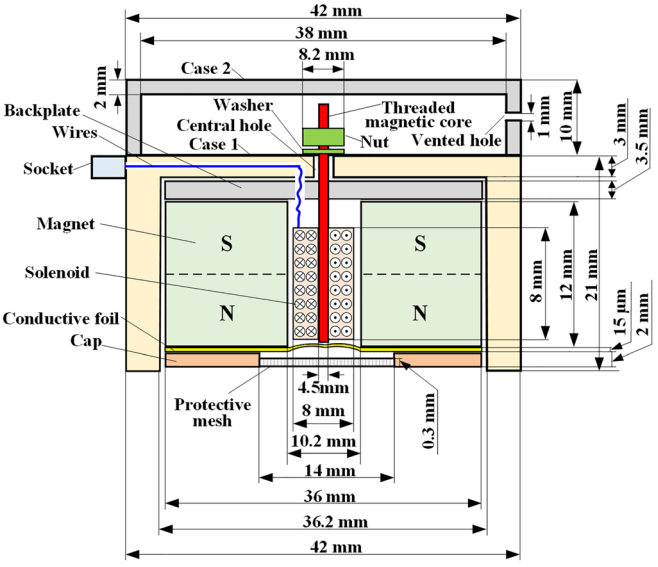

FIG. 2. Assembly schematic for a WEMDAT prototype (patent applied for).

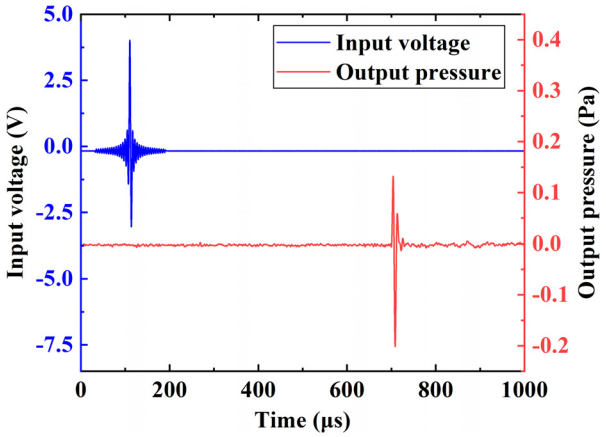

FIG. 3. Transmitted voltage signal from a WEMDAT (blue) and the corresponding detected pressure signal from a calibrated microphone at a distance of approximately 205.5 mm (red).

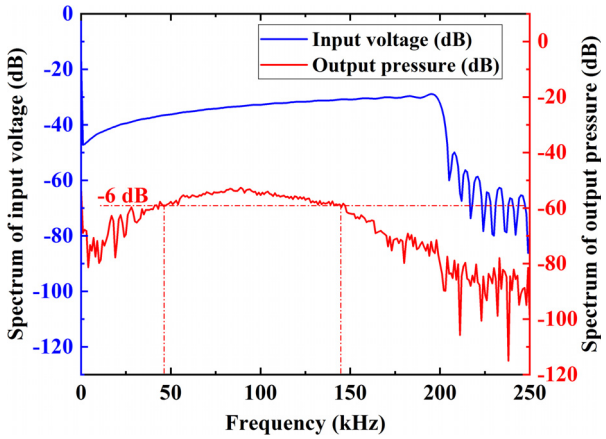

FIG. 4. Frequency spectra of the WEMDAT in the transmit mode and microphone in the receive mode.

The eddy current amplitude is sensitive to the lift-off distance between the solenoid and the foil. A slight increase in the lift-off will lead to an exponential drop of the eddy current amplitude,[19] significantly reducing transducer efficiency. Consequently, the smaller the lift-off, the higher the sensitivity of the WEMDAT. However, the lift-off distance should be greater than the vibration amplitude of the foil to avoid collision of the foil with the magnetic core and the solenoid during operation. A WEMDAT with a fixed lift-off distance may be desirable for applications with a single known input power level. The lift-off distance in the WEMDAT prototype can be adjusted by rotating the threaded magnetic core relative to the central holes of the backplate and case 1, and the position of the magnetic core and the solenoid can also be fixed by tightening the nut. Consequently, a series of optimum and stable static lift-off distances can be set for different input power levels, ensuring optimized transducer sensitivity. The edge of the foil is fixed between the cap and the magnet. Residual stresses in the foil have been minimized by applying a sufficiently large radial tension on its boundary during the assembly process, after which the foil adjacent to the inner surface of the magnet is formed into a dome-like shape, as shown in Fig. 2. This reduces the restoring force generated by the fixed boundary, which both enhances the vibration amplitude of the foil and forms the resultant acoustic field into a more focused radiation pattern.

The dimensions of a prototype WEMDAT design are shown in Fig. 2, where the length of the magnetic core is 27 mm, not shown in Fig. 2 for clarity. A 15 μm thick aluminium foil is chosen for the conductive foil of the WEMDAT. The ring magnet is an N45-grade NdFeB magnet with a remanence of 1.32 T. A mild-steel threaded rod with a diameter of 4.5 mm is chosen for the magnetic core, and an enamelled wire with a diameter of 0.1 mm is utilized for winding the solenoid, whose length, inner diameter, and outer diameter are approximately 6 mm, 5 mm (not shown in Fig. 2), and 6.5 mm, respectively.

A calibrated wideband microphone (B&K 4138-A-015) has been used to measure the generated sound pressure and the radiation pattern of WEMDAT prototypes. As the effective working frequency of the microphone is below 200 kHz, a sinc function signal with a frequency spectrum from 0 to 200 kHz is chosen as the driving signal. The WEMDAT is directly driven by a function generator (Tektronix AFG3102C), and the mathematical expression of the open-circuit voltage signal output by the generator is given by the following equation:

$$g(t) = A\mathrm{sinc}[2\pi f_0(t - t_0)], \tag{1}$$

where $f_0 = 200$ kHz, $t_0 = 79.2$ μs, and A = 10 V.

The peak-to-peak magnitude of the driving voltage across the WEMDAT is 7.1 V. A 0.2 Ω sampling resistor is fixed in series with the solenoid of the WEMDAT, and the peak-to-peak voltage over the resistor is 34.5 mV, corresponding to a peak-to-peak driving current of 172 mA. The microphone is positioned at a distance of 205.5 mm from the WEMDAT, and the protective mesh of the transducer has been removed to ensure that the dynamic characteristics are accurately measured. The driving voltage signal and the associated pressure signal detected by the microphone are shown in Fig. 3 for 128 time averages. The results show that the peak-to-peak pressure generated by the WEMDAT is 0.334 Pa. The duration of the pressure signal is short, around 22 μs with a sharp response profile which is due to the wideband characteristic of the transducer which produces a high measurement resolution in the time domain.

The frequency spectra of the input and output signals are shown in Fig. 4, where the centre frequency of the pressure signal is approximately 90.0 kHz with a −6 dB frequency bandwidth ranging from 46.4 kHz to 144.6 kHz. As the output power of the function generator reduces, the relationship between magnitude and frequency for the associated sinc function, represented by the blue curve in Fig. 4, becomes less uniform. This is because there is a 50 Ω output resistor inside the function generator, and the impedance of the WEMDAT increases with frequency, resulting in higher input voltages at high frequencies. Furthermore, the frequency response of the wideband microphone is not explicitly flat between 0 and 200 kHz.

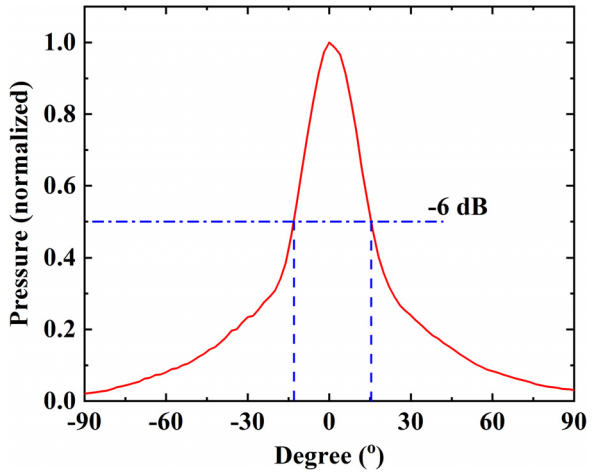

FIG. 5. Radiation pattern of a WEMDAT, driven by a 7.1 Vpp sinc function signal.

Consequently, the frequency spectrum of the pressure signal shown by the red curve in Fig. 4 is not directly attributable to the WEMDAT frequency response. However, it represents a reliable indicator of WEMDAT bandwidth. An accurate frequency response measurement can be obtained through deconvolution, provided that the frequency response of the microphone is known.

The radiation pattern of the WEMDAT is further measured using the wideband microphone system. The driving signal is the same as that shown in Fig. 3, with the measurement conducted at a distance of 205.5 mm. Assuming that the angle of the front face of the WEMDAT normal to the microphone is 0°, the WEMDAT is rotated from −90° to 90° in steps of 2°. The pressure signal amplitude is shown in Fig. 5. It is evident that the WEMDAT possesses a high level of acoustic directivity with a −6 dB half-beam divergence angle of approximately 14.2°. The radiation pattern is not precisely symmetric around 0°, attributable to errors introduced during the fabrication and measurement processes.

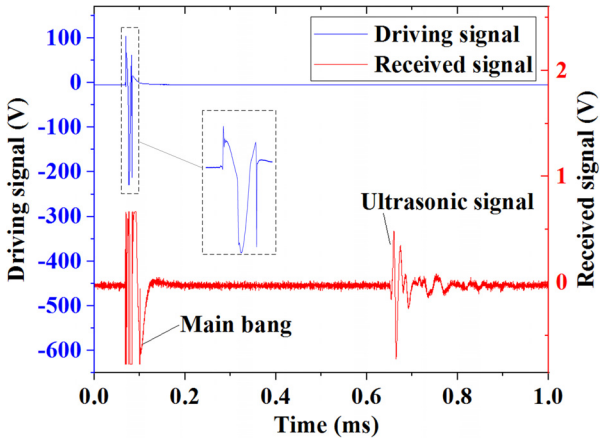

FIG. 6. Two WEMDATs operating in a pitch-catch configuration, showing the wideband driving voltage signal on WEMDAT1 (blue) and the received signal amplified by a broadband amplifier with a gain of 60 dB (red).

The final characterisation step determines the WEMDAT performance in a pitch-catch configuration, to assess WEMDAT performance in the receive mode. A second WEMDAT was fabricated for this step, where the separation distance for the measurement is approximately 201.0 mm. The transmitting WEMDAT (WEMDAT1) is driven by a pulser-receiver (Ritec RPR-4000), and the open-circuit voltage signal output by the pulser is a one-cycle sinusoidal tone burst signal with a centre frequency of 75 kHz. The peak-to-peak amplitude of the wideband driving voltage across WEMDAT1 is 336 V with a centre frequency of 65.2 kHz and a −6 dB frequency bandwidth from 12.5 kHz to 130.4 kHz. The peak-to-peak voltage across the integrated 0.2 Ω sampling resistor is 2.57 V, corresponding to a peak-to-peak driving current of 12.85 A. The signal received by the second WEMDAT (WEMDAT2) is amplified by a wideband receiver with a gain of 60 dB, and the driving and received voltage signals are shown in Fig. 6. The results indicate that the received signal is composed of a sharp pulse with high SNR in the time domain. Its −6 dB bandwidth in the frequency domain ranges from 42.9 kHz to 118.8 kHz. The results demonstrate the wideband performance of the WEMDAT operating as either a transmitter or a receiver.

The dynamic properties of the WEMDAT can be enhanced for practical applications. For example, the SNR in a receive mode can be significantly improved through a combination of high-sensitivity signal processing and tailored electronics. The transduction efficiency, frequency bandwidth, and radiation pattern can all be optimized through modifications to the WEMDAT assembly. Fundamentally, the WEMDAT exhibits a wideband characteristic which is vital for high precision ultrasound measurement applications. Furthermore, this wideband performance makes the WEMDAT an attractive and economic substitute for expensive conventional wideband microphone systems for the characterization of transduction efficiency, frequency bandwidth, and centre frequency of narrowband ultrasonic transmitters and also suitable as a standard acoustic source for the characterization of ultrasonic receivers. The ability of the WEMDAT to operate effectively as either a wideband transmitter or a receiver has been demonstrated, making it a highly versatile ultrasound measurement device potentially suitable for a wider range of applications, including ultrasonic communication, high audio-frequency loudspeakers, and the evaluation and characterization of conductive membranes.

This research was funded by EPSRC Grant No. EP/N025393/1.

REFERENCES

[1]S. Dixon, L. Kang, M. Ginestier, C. Wells, G. Rowlands, and A. Feeney, Appl. Phys. Lett. **110**, 223502 (2017).
[2]S. P. Kelly, G. Hayward, and T. E. G. Alvarez-Arenas, IEEE Trans. Ultrason. Ferroelectr. **51**, 1314 (2004).
[3]T. Wang, T. Kobayashi, and C. Lee, Micro Nano Lett. **11**, 558 (2016).
[4]D. E. Chimenti, Ultrasonics **54**, 1804 (2014).

[5]C. Li, D. Hutchins, and R. J. Green, IEEE Trans. Ultrason. Ferroelectr. **55**, 908 (2008).
[6]C. Li, D. Hutchins, and R. J. Green, IEEE Trans. Ultrason. Ferroelectr. **56**, 2060 (2009).
[7]W. Jiang and W. M. D. Wright, IEEE Trans. Ultrason. Ferroelectr. **64**, 1345 (2017).
[8]P. Pallav, T. H. Gan, and D. A. Hutchins, IEEE Trans. Ultrason. Ferroelectr. **54**, 1530 (2007).
[9]T. H. Gan, D. A. Hutchins, D. R. Billson, and D. W. Schindel, Ultrasonics **39**, 181 (2001).
[10]Y. Kusano, Q. Wang, G. L. Luo, Y. Lu, R. Q. Rudy, R. G. Polcawich, and D. A. Horsley, J. Microelectromech. Syst. **27**, 296 (2018).
[11]J. T. Garcia and T. G. Alvarez-Arenas, Elektron. Elektrotech. **22**(5), 89 (2016).
[12]A. Jimenez, A. Hernandez, J. Urena, M. C. Perez, F. J. Alvarez, C. D. Marziani, J. J. Garcia, and J. M. Villadangos, Sens. Actuators A-Phys. **148**, 342 (2008).
[13]M. H. Chen and M. S. C. Lu, J. Micromech. Microeng. **18**, 015009 (2008).
[14]D. W. Schindel and D. A. Hutchins, J. Acoust. Soc. Am. **97**, 1650 (1995).
[15]T. J. R. Eriksson, M. Laws, L. Kang, Y. Fan, S. N. Ramadas, and S. Dixon, Sensors **16**, 1363 (2016).
[16]A. Fartash, I. K. Schuller, and M. Grimsditch, J. Appl. Phys. **71**, 4244 (1992).
[17]L. Kang, S. Dixon, K. Wang, and J. Dai, NDT&E Int. **59**, 11 (2013).
[18]L. H. Cadwell, Am. J. Phys. **64**, 917 (1996).
[19]C. V. Dodd and W. E. Deeds, J. Appl. Phys. **39**, 2829 (1968).